Small-angle neutron scattering study on the morphology of seeded emulsion-polymerized latex particles*

M. P. Wai, R. A. Gelman, M. G. Fatica and R. H. Hoerl
Hercules Incorporated, Hercules Research Center, Wilmington, DE 19894, USA

and G. D. Wignall
National Center for Small-Angle Scattering Research, Oak Ridge National Laboratory, Oak Ridge, TN 37831, USA
(Received 5 May 1986; revised 25 August 1986; accepted 26 September 1986)

A statistical copolymer of styrene and methyl methacrylate was used as seed particles for further polymerization of trideuteromethyl (methyl-d_3) methacrylate in a starved monomer feed technique. The resulting polymer latex was shown to have a core/shell morphological structure as determined by small-angle neutron scattering. The overall size of the particle was in excellent agreement with the values obtained by light scattering and transmission electron microscopy.

(Keywords: neutron scattering; core/shell; latex morphology; seeded emulsion particles; latex structure)

INTRODUCTION

Polymerization of latex particles has been studied for a number of years. More recently, emulsion polymerization research has focused on the preparation of latex copolymer with radial compositional gradients. The structure of composite polymer particles prepared by seeded emulsion polymerization procedures has been considered by a number of investigators. The proposed core/shell latex polymerization mechanism is not widely accepted and the same evidence has been used to argue both for and against it. Grancio and Williams[1] proved, using kinetic, morphology and swelling data, a core/shell structure in which the growing latex particle consisted of a polymer-rich core surrounded by a monomer-rich shell that served as the major locus of polymerization. Vanderhoff *et al.*[2] used electron microscopy staining techniques to consider particle morphology. They showed a core/shell type structure which appeared to be dependent on the method of polymerization. Okubo *et al.*[3] found that the morphology changes with age. Soap titration methods have been used in a report that suggests the formation of a core/shell structure[4]. It has been reported[5] that, although emulsion polymerization generally produces perfect spherical particles, seeding techniques lead to the formation of anomalous particle shapes[6], including particles containing voids. Min *et al.*[7] correlated the storage stability of composite particles with the amount of graft copolymer formed during the seeded emulsion polymerization. Lee *et al.*[8] used electron microscopy and surface group titration to conclude that an inversion of the first and second stage polymer can occur. They propose a range of morphologies from droplets of one polymer within the other to a well defined core/shell structure depending on relative hydrophilicity and the extent of phase separation between two polymers.

Small-angle neutron scattering (SANS) has been used to characterize the dimensions of individual polymer molecules in the bulk phase. The requirements of this experimental technique appear ideally suited to the determination of the morphology of the above described materials based on the assumption that the deuterated tagged molecules are chemically identical and compatible with their hydrogenous analogues. In most cases this assumption is valid if the polymer is non-crystalline and the phenomenon of interest is not critically dependent on the glass transition temperature of the polymer. For very high-molecular-weight systems, demixing of fully deuterated and protonated species has been observed in the melt[9,10]. Demixing is believed not to occur in this study because of the modest molecular weight of the components and because the labelled chains are only partially deuterated.

Goodwin *et al.*[11] have used neutron scattering to determine latex particle sizes and to study the effects of monomer-induced swelling. It has been reported that a polymerization process involving a seed nucleus gives rise to a core/shell morphology[12]. O'Reilly *et al.*[13] employed SANS to study the core/shell morphology of pure polystyrene latexes by incorporating perdeuterated styrene and perdeuterated methyl methacrylate monomers in the polymerization; and more recently, Cebula *et al.*[14] investigated the core/shell morphology of hydrogenated and perdeuterated methyl methacrylate.

In this paper, we present our SANS study of the polymer particle morphology formed by polymerization of trideuteromethyl (methyl-d_3) methacrylate in the presence of a well characterized core of hydrogenated (50/50) poly(styrene-*co*-methylmethacrylate) seed. A core/shell structure is proposed for these composite particles whose incompatible stage 1 and stage 2 polymers have similar glass transition temperatures.

* Hercules Research Center Contribution number 1896

0032-3861/87/060918-05$03.00

EXPERIMENTAL

Trideuteromethyl (methyl-d_3) methacrylate

Perdeuteromethanol was slowly added to a stirred, chilled solution of methacryloyl chloride and triethylamine in anhydrous diethyl ether. A 5% molar excess of the acid chloride and amine were used. When the methanol addition was complete, the mixture was warmed, filtered and the precipitate washed with excess ether. The ether solution was extracted three times with 5% aqueous hydrochloric acid. Extraction with aqueous sodium bicarbonate was repeated until the aqueous layer was basic. The organic layer was separated, dried over magnesium sulphate and concentrated by rotary evaporation under aspirator vacuum. The concentrate was purified by a simple distillation. The product was determined to be more than 99% pure by proton n.m.r. and was stored with 50 ppm tert-butylcatechol at 3°C.

Preparation of latexes

Monomers were used without purification or inhibitor removal. Styrene and methyl methacrylate were purchased from Aldrich Chemical Company. Deionized and deoxygenated water was used for all polymerizations. Ammonium peroxydisulphate (Eastman) and sodium lauryl sulphate ('Sipon WD' 98%, Alcolac, Inc.) were used as received.

Polymerizations were conducted in a 0.5 litre cylindrical jacketed reaction flask equipped with reflux condenser, Teflon stirrer paddle, two injection ports, thermometer and nitrogen inlet and outlet (through the condenser).

Seed latex preparation

To the nitrogen-purged reactor, 210 g water, 0.12 g sodium lauryl sulphate and 0.05 g initiator (ammonium peroxydisulphate) were charged. The contents were purged with nitrogen, while stirring, and the temperature was brought to 70°C over 20 min. A monomer mixture, 25 g each of styrene and methyl methacrylate, was next added to the reactor simultaneously with a separate addition of 0.19 g of sodium lauryl sulphate and 0.015 g initiator dissolved in 50 g of water. Both feeds were added to the reactor at constant rates over 20 min. When the addition was complete, 0.2 g initiator was added to the reactor and the temperature maintained with stirring for an additional 30 min. The latex was then cooled by passing cold water through the reactor jacket and bottled for storage.

Seeded emulsion polymerization

To the reactor set-up as described above, 105 g of seed latex (16.2% total solids) was charged. The seed latex was brought to 70°C with stirring and nitrogen purge. Methyl-d_3 methacrylate (17 g) was added next over 8 min. The latex was maintained at 70°C with stirring for an additional 30 min, then cooled immediately and stored in glass bottles. The two samples of interest are listed in *Table 1* along with their respective calculated neutron scattering cross-section areas.

Small-angle neutron scattering

The proper mixture of deuterium oxide and water needed to contrast-match the core was calculated to be 25% deuterium oxide. For the core material, pure D_2O was used. Sample concentration was 10 wt% and was enclosed in a disc-like quartz cell of 1 or 2 mm path length.

The neutron experiments were performed in a 30 m small-angle neutron scattering facility at the National Center for Small-Angle Scattering Research, Oak Ridge National Laboratory. A description of the apparatus has been published elsewhere[15,16]. The incident beam, of wavelength $\lambda = 4.74$ Å ($\Delta\lambda/\lambda = 6\%$), was collimated by a source slit (1.7 cm diameter) and a sample slit (0.9 cm diameter), separated by a distance of 7.6 m. The area detector (64 × 64 cm^2) was placed at a sample-to-detector distance (*SDD*) of 18.9 m. This gives a scattering vector (q) range of $0.003 < q < 0.0225$ Å^{-1}. Typical runs consisted of sample scattering and then correction for instrumental background, parasitic scattering and detector sensitivity. All scattering was normalized for sample thickness, transmission and incident beam flux[17]. Calibration of the data was accomplished by means of a precalibrated irradiated aluminium standard containing ~0.7 vol% voids, which had in turn been calibrated by use of the incoherent scattering of water and vanadium and the coherent scattering of partially labelled blends of monodisperse polystyrene[15]. The data were converted to an absolute differential scattering cross section per unit solid angle per unit volume, $d\Sigma(q)/d\Omega$, in units of cm^{-1}. A typical two-dimensional contour plot is shown in *Figure 1*, and, as all samples showed cylindrical symmetry about the incident beam, the data were radially averaged. In view of the large particle size of the latexes studied, it is important to consider instrumental resolution effects resulting from the finite resolution of the detector

Table 1 Samples used in this study

Sample	Composition	Neutron scattering length density (cm^{-2})
A	PS/PMMA (50:50)	0.116×10^{11}
B	Core: PS/PMMA (50:50)	0.116×10^{11}
	Shell: PMMA-d_3	0.332×10^{11}

PS = polystyrene
PMMA = poly(methyl methacrylate)
PMMA-d_3 = poly(methyl-d_3 methacrylate)

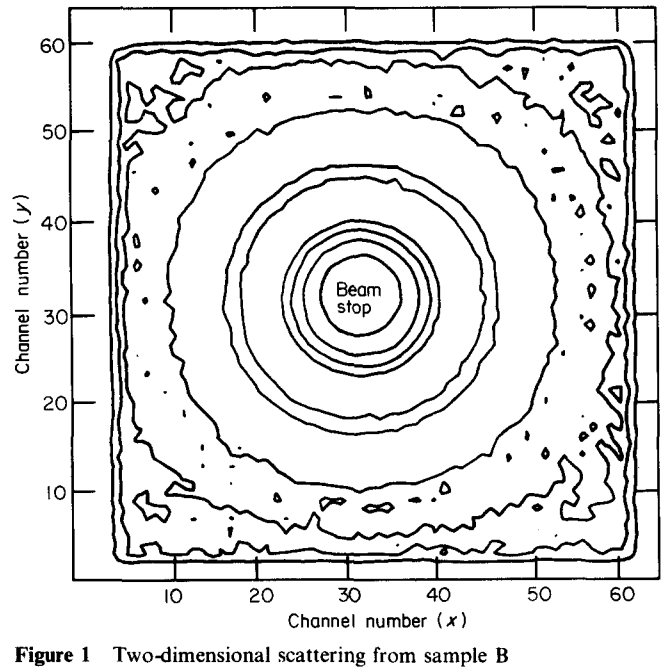

Figure 1 Two-dimensional scattering from sample B

elements, the wavelength spread of the incident beam ($\Delta\lambda/\lambda \sim 6\%$) and the angular divergence of the incident and scattered beams determined by the sizes of the sample and source slits. The mathematical procedures for the desmearing process have been discussed by Glatter[18] and Moore[19]. These cannot be desmeared directly because the data are subject to statistical errors and because they are incomplete. The lower-angle portion of the data ($q < 0.003$ Å^{-1}) is missing because of the finite size of the beamstop and the higher-angle region is missing because of poor signal-to-noise ratio as the data fall rapidly with q at higher angles. The algorithm used here was the one developed by Moore[19] and applied to the particular geometry of the 30 m instrument by Ramakrishnan[20]. In addition to giving the desmeared intensity curve, the method gives the radius of gyration R_g, the zero-angle cross section $d\Sigma(0)/d\Omega$, and the maximum dimensions of the particles even though data were not collected in the true Guinier range ($gR_g < 1$). These parameters agree very well with the values obtained by other methods and confirm the core/shell structure of the latices.

ANALYSIS OF SANS DATA

The coherent elastic differential scattering cross section of a solution of scattering particles can be expressed as:

$$d\Sigma(q)/d\Omega = (n_1 - n_2)^2 N_v V_p^2 P(q) \quad (1)$$

where n_1 and n_2 are the scattering length densities of the particle and solvent, respectively, N_v is the number of particles per unit volume, V_p is the particle volume, $P(q)$ is the particle form factor, which describes the scattering profile, and q is the scattering vector defined as:

$$q = (4\pi/\lambda)\sin\theta \quad (2)$$

where λ is the wavelength of the incident neutron beam and 2θ is the scattering angle. The particle form factor for an isotropic solid sphere of uniform radius has been solved by Rayleigh[21] as:

$$P(q) = \frac{9[\sin(qR) - qR\cos(qR)]^2}{q^3R^3} \quad (3)$$

where R is the radius of the sphere.

The particle form factor for a hollow sphere has been solved by Pecora and Aragon[22] as:

$$P(q) = \frac{9}{x^4(1-l^3)^2}\left(\frac{\sin x}{x}\frac{\sin(xl)}{x} - \cos x + l\cos(xl)\right)^2 \quad (4)$$

where $l = R_i/R_a$, R_i is the radius of the inner particle and R_a is the radius of the outer particle and $x = qR_a$. At $l = 0$, this hollow-sphere scattering function reduces to the solid-sphere scattering function.

Equation (4) was derived for a completely monodispersed system. In general, colloidal particles are seldomly monodispersed and allowance has to be made for the spread of particle sizes. Owing to dispersion of the particle size, it is necessary to employ a particle distribution function to account for this deviation from ideality. In this work, a zeroth-order log-normal (ZOLD) probability distribution was used of the form[23]:

$$P(R) = \frac{1}{2(\pi^{1/2}\sigma_0 R_m \exp(\sigma_0/2)}\exp\left(\frac{-(\ln R - \ln R_m)^2}{2\sigma_0}\right) \quad (5)$$

where R_m is the modal mean radius and σ_0 is a measure of the width and skewness of the distribution given by:

$$R_m(\exp(4\sigma_0)^2\exp(3\sigma_0)^2)^{\frac{1}{2}} \quad (6)$$

RESULTS

Figures 2 and *3* show the radial averaged plots of the scattering from samples A and B, respectively. Note that after correction for instrumental broadening, the valleys and peaks are greatly sharpened. Equation (4) was used, with the employment of the distribution functions, to fit the scattering curves. The fitting procedure used was a steepest-descent non-linear minimization employing the method of ridge analysis[24]. It was found that sample A was best fitted with a solid-sphere scattering function and sample B with a hollow-sphere scattering function. The results of these fits are shown in *Figures 4* and *5* for samples A and B, respectively. *Table 2* lists the results along with the mean and distribution of the particle sizes. The differences in the radius of the two materials are within the experimental error of the analysis.

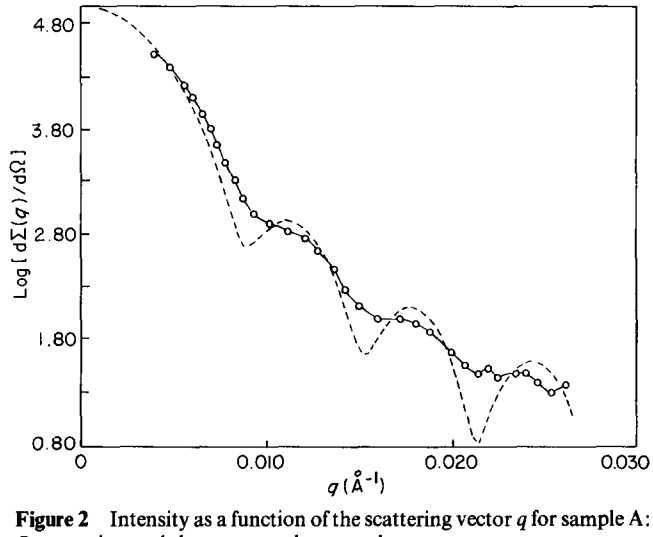

Figure 2 Intensity as a function of the scattering vector q for sample A: ○, experimental data; -----, desmeared curve

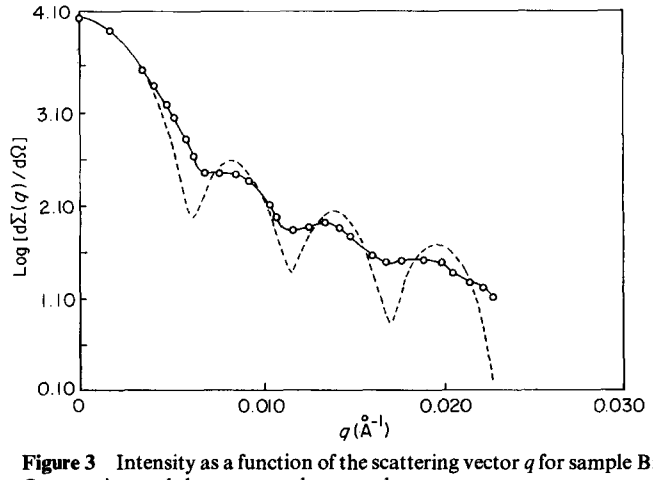

Figure 3 Intensity as a function of the scattering vector q for sample B: ○, experimental data; -----, desmeared curve

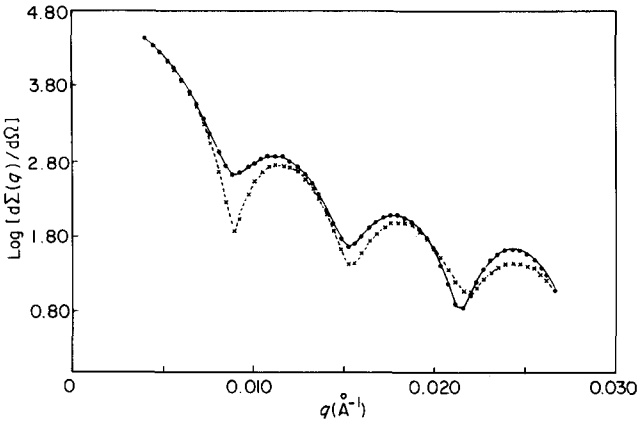

Figure 4 Fitting of scattered intensity with a distribution function (ZOLD) for sample A: —●—, desmeared experimental data (from *Figure 2*); -- × --, fitted by ZOLD

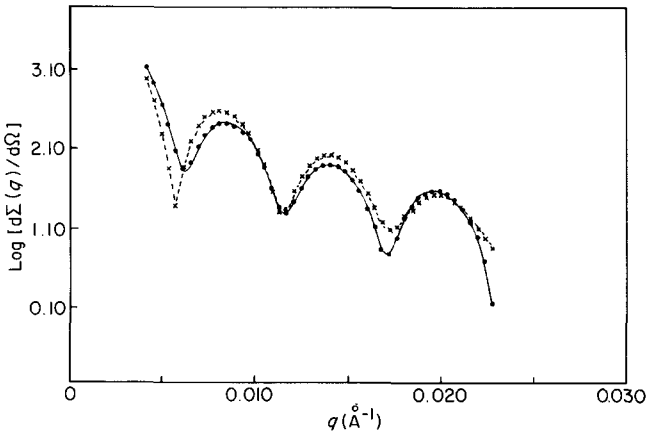

Figure 5 Fitting of scattered intensity with a distribution function (ZOLD) for sample B: —●—, desmeared experimental data (from *Figure 3*); -- × --, fitted by ZOLD

DISCUSSION

Best results were achieved by fitting a solid-sphere scattering function to sample A and hollow-sphere scattering function to sample B. The parameters used are consistent with the known dimensions of the samples, based upon stoichiometric calculations. The calculation yields a ratio of the core plus shell radius to the core radius of 1.3, which is consistent with the experimental SANS result of 1.2 (see *Table 3*). These results are consistent with the composition of the samples as described in *Table 1*. Data for sample A, fit best by a solid-sphere scattering function, is a solid-sphere composed of a random copolymer of polystyrene and poly(methyl methacrylate). Fitting the data obtained for sample B to a hollow sphere, i.e. the shell region of a core/shell structure, supports our concept of a composite core/shell structure formed by the seeded emulsion polymerization.

The results of the fitting procedure gave a shell size of 14 nm with a mean distribution of 6 nm. This wide variation in the width of the shell indicates that it is in the latter stages of polymerization where the greater variation in the size of the particles occurs. It is noted, however, that the variation is not significantly greater than that for the other neutron scattering data. Based on these dimensions obtained from the ZOLD fitting procedure, the radius of gyration R_g and the zero-angle scattering cross section $d\Sigma(0)/d\Omega$ may be calculated for both the core and core/shell latexes. The results are shown in *Table 2* and indicate that the proposed core/shell structure and dimensions are consistent, not only with the observed R_g, but also with the absolute magnitude of the measured zero-angle cross section, within the experimental errors.

The overall size of these particles has also been determined by transmission electron microscopy and light scattering. These results are shown in *Table 3*, which lists the overall diameter. As can be seen, there is close agreement between the data obtained by microscopy and light scattering and those obtained by neutron scattering. This confirms that the particle dimensions calculated from the neutron scattering data are consistent with other techniques.

It is interesting that the interconsistency of the model data with microscopy, stoichiometry and the absolute SANS calibration was achieved using relatively high concentrations (10 wt %) of latex particles. Calculations[25] indicate that the measured R_g and zero-angle cross section $d\Sigma(0)/d\Omega$ are strongly affected by the concentration of scattering particles when the data are analysed only at low q in the Guinier region. In contrast to this procedure, the data reported above were analysed by indirect Fourier transform methods[20], which make use of data in the whole measured q range. This makes the analysis much less sensitive to concentration effects which are exhibited predominantly at low q, making R_g and $d\Sigma(0)/d\Omega$ virtually independent of concentration in the range studied[26].

Table 2 Results of SANS analysis

(a) Best model fit to experimental (desmeared) SANS data (see *Figures 4* and *5*)

Sample	Radius size (Å) from zeroth-order log-normal (ZOLD)
A: Core	$\bar{r}=505\pm46$
B: Core	$\bar{r}=475\pm42$
Shell	$\bar{r}=143\pm64$

(b) Calculated and observed parameters from desmearing routines using above core and shell dimensions

	Observed via desmearing		Calculated using above dimensions	
Sample	R_g (Å)	$d\Sigma(0)/d\Omega$ (cm^{-1})	R_g (Å)	$d\Sigma(0)/d\Omega$ (cm^{-1})
A: Core in D_2O	391 ± 20	$(91\pm20)\times10^3$	401 ± 20	$(123\pm20)\times10^3$
B: Core/shell (core contrast-matched)	527 ± 25	$(14\pm2)\times10^3$	554 ± 25	$(14\pm2)\times10^3$

Table 3 Comparison of SANS results with other techniques

	Mean diameter (Å)		
Sample	SANS[a]	TEM[b]	LS[c]
A: Core	1010 ± 50	900 ± 90	1120 ± 112
B: Core and shell	1200 ± 60	1070 ± 107	1300 ± 130

[a] Small-angle neutron scattering (this work)
[b] Transmission electron microscopy
[c] Light scattering data. Particle size measured using a Coulter Nanosizer

CONCLUSIONS

Latices prepared by the seeded emulsion polymerization process described here have a core/shell structure. The core, of radius approximately 50 nm, is surrounded by a shell of radius 14 ± 6 nm. The variation in the thickness of the shell is consistent with its being formed during the latter stages of polymerization. These results imply that material formed during the latter stages of polymerization does not migrate to the interior of the particle. This work also verifies that SANS is a useful technique for studying the structure of latexes.

ACKNOWLEDGEMENTS

We are grateful for the assistance of V. Ramakrishnan who developed desmearing procedures adapted to the geometry of the 30 m SANS instrument. We thank Dr R. E. Cohen for stimulating discussions and suggestions.

Research sponsored by Hercules Incorporated and the National Science Foundation under Grant DMR-77 24459 with the US Department of Energy under Contract DE-AC05-840R21400 with Martin Marietta Energy Systems Inc.

REFERENCES

1 Grancio, M. P. and Williams, D. J. *J. Polym. Sci.* (*A*-1) 1970, **8**, 2617
2 Misra, S. C., Pichot, C., El-Aasser, M. S. and Vanderhoff, J. W. *J. Polym. Sci., Polym. Lett. Edn.* 1969, **17**, 567
3 Okubo, M., Ando, M., Yamada, A., Katsuta, Y. and Matsumoto, T. *J. Polym. Sci., Polym. Lett. Edn.* 1980, **18**, 481
4 Okubo, M., Yamada, A. and Matsumoto, T. *J. Polym. Sci., Polym. Chem. Edn.* 1980, **16**, 3219
5 Okubo, M., Ando, M., Yamada, A., Katsutu, Y. and Matsumoto, T. *J. Polym. Sci., Polym. Lett. Edn.* 1981, **19**, 143
6 Trent, J. S., Scheinbeim, J. I. and Couchman, P. R. *J. Polym. Sci., Polym. Lett. Edn.* 1981, **19**, 315
7 Min, T. I., Klein, A., El-Aasser, M. S. and Vanderhoff, J. W. *J. Polym. Sci., Polym. Chem. Edn.* 1983, **21**, 2845
8 Lee, D. I. and Ishikawa, T. *J. Polym. Sci., Polym. Chem. Edn.* 1983, **21**, 147
9 Bates, F. S., Wignall, G. D. and Koehler, W. C. *Phys. Rev. Lett.* 1985, **55**, 2425
10 Bates, F. S. and Wignall, G. D. *Macromolecules* in press
11 Goodwin, J. W., Ottewill, R. H., Harris, N. M. and Tabony, J. *J. Colloid Interface Sci.* 1980, **78**, 253
12 Hasan, S. M. *J. Polym. Sci., Polym. Chem. Edn.* 1982, **20**, 3031
13 O'Reilly, J. *et al.*, 'Proceedings of AIChE Meeting', Houston, March 1983
14 Cebula, D. J., Goodwin, J. W., Ottewill, R. H., Jenkin, G. and Tabony, J. *Colloid Polym. Sci.* 1983, **261**, 610
15 Wignall, G. D., Hendricks, R. W., Koehler, W. C., Lin, J. S., Wai, M. P., Thomas, E. L. and Stein, R. S. *Polymer* 1981, **22**, 886
16 Koehler, W. C. *et al.* in 'Scattering Techniques Applied to Supramolecular and Nonequilibrium Systems', (Eds. S. H. Chen and R. Nossal), Plenum Press, New York, NATO Adv. Stud. Ser. 1981, Vol. 83, p. 35
17 National Center for Small-Angle Scattering Research, 'Users Guide', Oak Ridge National Laboratory, 1985
18 Glatter, O. *J. Appl. Cryst.* 1977, **18**, 87
19 Moore, P. B. *J. Appl. Cryst.* 1980, **13**, 168
20 Ramakrishnan, V. *J. Appl. Cryst.* 1985, **18**, 42
21 Rayleigh, Lord *Proc. R. Soc. Lond. A* 1911, **84**, 24
22 Pecora, R. and Aragon, S. R. *Chem. Phys. Lipids* 1974, **13**, 1
23 Kerker, M. 'The Scattering of Light and Other Electromagnetic Radiation', Academic Press, New York, 1969
24 Hoerl, A. E. *Chem. Eng. Prog. Symp. Ser.* 1964, **60**, 67
25 Hayter, J. B. and Penzold, J. *Colloid Polym. Sci.* 1983, **261**, 1023
26 O'Reilly, J., private communication